Biomedical Signal Processing and Control 78 (2022) 104014

Contents lists available at ScienceDirect

Biomedical Signal Processing and Control

journal homepage: www.elsevier.com/locate/bspc

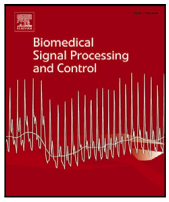

Respiratory analysis during sleep using a chest-worn accelerometer: A machine learning approach

Franziska Ryser [a,b,e,*,1], Simon Hanassab [a,c,d,1], Olivier Lambercy [a], Esther Werth [b,e,2], Roger Gassert [a,2]

[a] Rehabilitation Engineering Laboratory, ETH Zurich, Zurich, Switzerland
[b] Department of Neurology, University Hospital Zurich, University of Zurich, Zurich, Switzerland
[c] Department of Electrical and Electronic Engineering, Imperial College London, London, United Kingdom
[d] UKRI Centre for Doctoral Training in AI for Healthcare, Imperial College London, London, United Kingdom
[e] Sleep and Health Zurich (SHZ), University of Zurich, Zurich, Switzerland

ARTICLE INFO

Keywords:
Accelerometer
Machine learning
Respiratory rate
Sleep diagnostics
Sleep-related breathing disorders

ABSTRACT

Objective: There is a great interest in observing breathing patterns during sleep, as sleep disturbances can be caused by respiratory irregularity and cessations. In this paper, we introduce the first steps to an accelerometer-based screening tool for respiratory rate estimation and a novel approach towards detecting breathing cessations such as apnea/hypopnea, by extending and combining established signal processing routines with machine learning.

Methods: From a single chest-worn accelerometer, we estimate the respiratory rate based on the inhalation/exhalation movements of the chest and carry out a full overnight validation. On this basis, we build a set of features customized to detect irregular respiratory activity, including a novel feature: the respiratory peak variance (RPV). From thirteen healthy subjects, a classification model was trained, validated, and tested with over 98 h of PSG-labeled accelerometer data.

Results: The algorithm estimated the respiratory rate with a mean difference of 1.8 breaths per minute compared to respiratory inductance plethysmography during overnight PSGs. The machine learning classifier detected respiratory cessations with a sensitivity and specificity of 76.05% and 70.05% respectively, with an overall accuracy of 70.95%.

Conclusion: We successfully demonstrated the potential of a novel respiratory feature set in a preliminary application with young healthy volunteers for respiratory rate estimation and in identifying apnea/hypopnea events during overnight sleep.

Significance: We present a simple and unobtrusive wearable system that can serve as a home screening tool for sleep-related breathing disorders.

1. Introduction

Sleep is central to the maintenance of body function. Sleep disturbances caused by endogenous or exogenous factors manifest themselves as short arousal reactions or awakenings which fragment otherwise consolidated sleep patterns. Such arousals can be caused by respiratory cessations including complete (apnea), or incomplete (hypopnea) obstructions of the airways, which in turn reduce sleep quality. An irregular respiratory rate (RR) often correlates with the presence of breathing cessations during sleep [1,2]. Therefore, there is a great interest in observing breathing characteristics such as RR in order to distinguish obscure breathing patterns during sleep. In a laboratory setting, the gold standard for comprehensive breathing analysis during sleep is a fully supervised polysomnography (PSG) routine, including measurements of brain activity, oxygen level, breathing functions, respiratory airflow, and limb movements [3]. This routine, however, is relatively complex, cumbersome, and associated with high financial and time-related costs. Furthermore, the unnatural sleeping environment can cause white-coat syndrome and first-night effects, thus masking the authenticity of regular sleep experienced at home [4]. Unattended PSGs or routines with a reduced number of channels, such as respiratory

* Corresponding author at: Rehabilitation Engineering Laboratory, ETH Zurich, Zurich, Switzerland.
E-mail address: relab.publications@hest.ethz.ch (F. Ryser).
[1] F. Ryser and S. Hanassab contributed equally to this work.
[2] E. Werth and R. Gassert contributed equally to this work.

https://doi.org/10.1016/j.bspc.2022.104014
Received 18 November 2021; Received in revised form 15 May 2022; Accepted 11 July 2022
Available online 6 August 2022
1746-8094/© 2022 The Author(s). Published by Elsevier Ltd. This is an open access article under the CC BY license (http://creativecommons.org/licenses/by/4.0/).

polygraphy (RP), and automatic processing routines allow for less expensive home assessments [5,6]. These assessments, however, normally encompass only a single night of recording, thereby neglecting the night-to-night variability present in natural sleep [7]. In order to establish a more encompassing approach, an alternative method is needed to monitor respiration during sleep, with reduced device and electrode attachments to enable home monitoring over several nights.

Wearable accelerometers have been introduced as a potential non-invasive alternative to PSGs. Body-worn sensors, for example, measure the displacement of the thorax [8,9] where the respiratory rate (RR) is estimated [10–16]. Accelerometers have, in a more complex setup, even be used to estimate the airflow [17]. Dehkordi et al. tested the method to be robust in different positions (supine, prone, and left side) while lying awake in bed [12]. More recently, advanced signal processing techniques to estimate the RR in ICU patients were presented by Jarchi et al., reporting encouraging results with a maximum mean difference of +2.56 breaths per minute (bpm) compared to a photoplethysmography Ref. [13]. Although the literature is promising, it reveals only few validatory efforts of RR estimations during sleep. Morillo et al. reported RR deviations within the range of +2.11/−3.05 bpm with an accelerometer positioned on the suprasternal notch benchmarked against overnight PSG routines [11]. Full overnight validation of RR estimation with a chest-worn accelerometer during sleep remains to be shown.

For a full characterization of sleep quality, there is a strong need to extend the analysis of respiratory signals beyond solely detecting the RR. More sophisticated methods have been introduced using alternative sensing methods compared to PSG routines [18–23], namely machine learning techniques to automatically identify apnea/hypopnea events. Van Steenkiste et al. presented a deep-learning approach with bio-impedance signals from the chest. In 25 patients, they classified apnea/hypopnea events with an accuracy of 72.8% against the gold standard PSG [24]. Pépin et al. tested a head-mounted system measuring mandibular movements, exhibiting a two-class discrimination between patients with a high or low Respiratory Disturbance Index with an accuracy of 88% [25]. Interpretations, nonetheless, from both these studies prove challenging since no substantial insights were reported as to how well their algorithms detect individual respiratory events, nor the chosen classification features.

The aim of our study was to develop an accelerometer-based screening tool to discriminate between two encompassing types of respiratory events. We placed an accelerometer sensor onto the sternum to monitor the regularity of respiratory activity and hypothesized that features drawn from the accelerometer signals are adequate in deducing the presence of breathing cessations during sleep.

We introduce a novel set of signal features customized for this purpose, and show its potential by training a machine learning classification model which automatically detects breathing cessations during overnight sleep. This work is of value because it is the first to perform a full overnight validation of RR estimation from a chest-worn accelerometer during sleep, and harness this with further breathing characteristics to automatically detect breathing cessations. Our model contributes to the establishment of new assessments of disrupted respiratory events, with potential applications in the comfort of one's own known home environment. With this approach, we aim to support efforts to provide earlier diagnosis of sleep-related breathing disorders (SRBDs), and thus grant more people access to the timely treatment they require.

2. Materials & methods

In this work, we apply a machine learning approach for the detection of irregular breathing cessations during sleep, such as apnea/hypopnea events, with a chest-worn accelerometer. First, we calculated the RR and validated its reliability against a PSG reference during nearly 90 h of overnight sleep from twelve healthy subjects. Indeed, even healthy subjects may occasionally have disrupted respiration (apnea/hypopnea events of five or less per hour are considered normal). Second, we investigated the potential of the RR to automatically detect respiratory events which disrupt regular sleep. For the purposes of this paper, we describe this phenomenon as disrupted breathing, or otherwise characterized as regular (uninterrupted) breathing.

Table 1
Subject demographics (BMI: Body Mass Index; ESS: Epworth Sleepiness Scale; AHI: Apnea-Hypopnea Index; TiB: Time in Bed; on bottom row: mean value ± standard deviation; Σ(S): total number of subjects).

Subject	Sex	Age	BMI	ESS	AHI [# / h]	TiB [h]
S_01	M	33	23.2	4	0.3	7.3
S_02	F	21	22.2	5	0.1	7.6
S_03	F	29	21.3	1	0.3	7.3
S_04	F	28	24.8	7	0.3	7.9
S_05	M	25	22.7	1	0.5	8.5
S_06	M	25	21.1	9	0.2	7.6
S_07	M	24	23.2	1	1.5	7.2
S_08	M	26	23.1	6	14.8	8.0
S_09	F	27	20.9	8	0.1	8.1
S_10	M	19	19.5	6	0.2	7.8
S_11	F	30	20.1	6	0.2	7.3
S_12	F	19	24.0	7	0.9	7.4
S_13	M	27	19.6	13	0.3	6.7
Σ(S) = 13	**7M; 6F**	**25.6 ± 4.0**	**22.1 ± 1.6**	**5.7 ± 3.3**	**1.5 ± 3.9**	**7.6 ± 0.4**

2.1. Study participants and protocol

Data were collected from thirteen healthy subjects (7M; 6 W), between the ages of 19 and 33. All participants had no pre-existing conditions, reported a regular sleep rhythm with a bed-time between 10 pm and 12 am, and were neither addicted to nicotine nor caffeine. Daytime sleepiness was recorded with the Epworth Sleepiness Scale – a qualitative questionnaire where scores above ten indicate increased daytime sleepiness [26]. Full subject demographics are outlined in Table 1. Each subject partook in a single night standard PSG routine in the sleep laboratory at the University Hospital Zurich. The PSG routines served as screening nights for healthy subjects to rule out hidden somatic sleep disorders in advance of the main study project (data presented elsewhere).

Upon arrival, subjects were screened with standard sleep questionnaires and equipped with the accelerometer sensor and electrodes. Lights-off was adjusted to their usual bedtime, and their 'Time in Bed' was set to around seven hours. To describe sleep behavior in our healthy population, the Apnea-Hypopnea Index (AHI) was extracted from the PSG data. The AHI outlines categorizations widely used as part of clinical respiratory classifications [27]. It indicates the averaged number of apnea and hypopnea events observed per hour of sleep whereby an AHI score of greater than fifteen in adults is considered clinically relevant [27]. One subject (S_08) exhibited a near-to-moderate AHI score, however, individuals with healthy sleeping patterns can similarly exhibit characteristic respiratory cessations sporadically, albeit with a reduced frequency, which would not usually require medical attention [2]. Full ethics approval was received from the Swiss cantonal ethics committee (ClinicalTrials.gov Identifier: NCT03356938). All participants gave written informed consent to partake in the study.

2.2. Sensor systems

For this study, the PSG routine was carried out using a commercial PSG bio-signal amplifier (Embla N7000, Natus, Colorado, USA). Eight electroencephalography (EEG) electrodes (F3, F4, C3, C4, O1, O2, and two mastoid electrodes M1 and M2), binocular electrooculography, and two leads of chin electromyography were derived. Respiratory activity was assessed with two respiratory inductance plethysmography

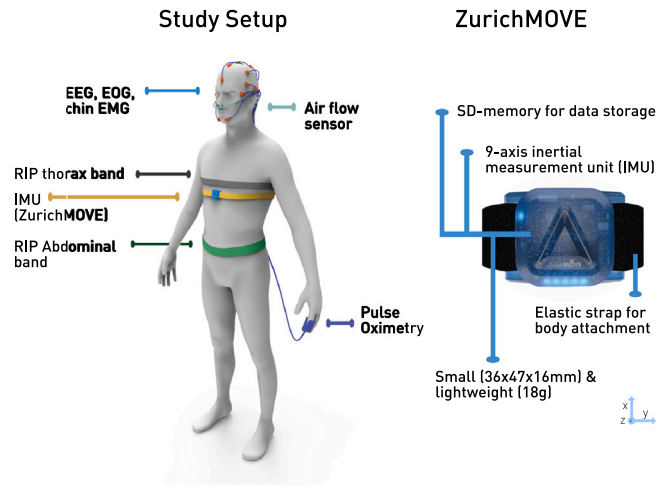

Fig. 1. On the left, the polysomnography (PSG) setup is shown, including electroencephalography (EEG), electrooculography (EOG), and chin electromyography (EMG) for sleep detection, as well as respiratory inductance plethysmography (RIP) to measure the respiration rate. The ZurichMOVE sensor with an internal intertial measurement unit (IMU) strapped around the chest measures the displacement of the thorax. On the right, the ZurichMOVE sensor, used here as an accelerometer, is shown.

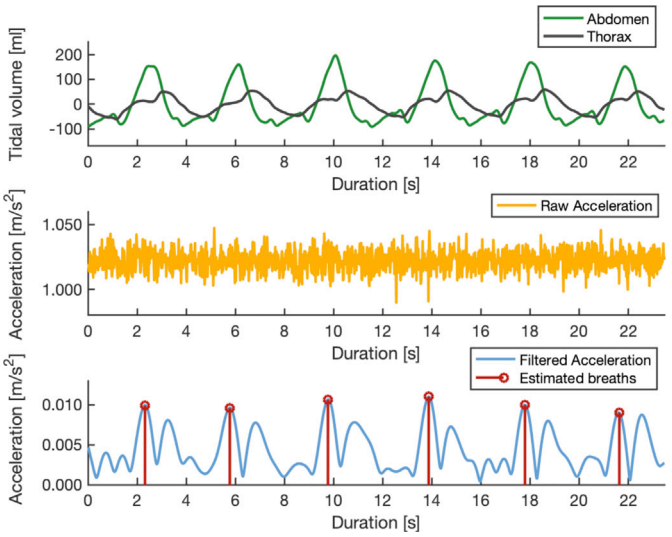

Fig. 2. The signal processing pipeline shown on a representative sample of 23 s. At the top, the polysomnography (PSG) reference is shown as the respiratory inductance plethysmography (RIP) abdomen (green) and thorax (gray) signals. The raw acceleration signal magnitude of the corresponding time is shown in yellow. On the filtered and noise-thresholded signal (blue), a peak-finder approach finds the individual inspiratory events (in red).

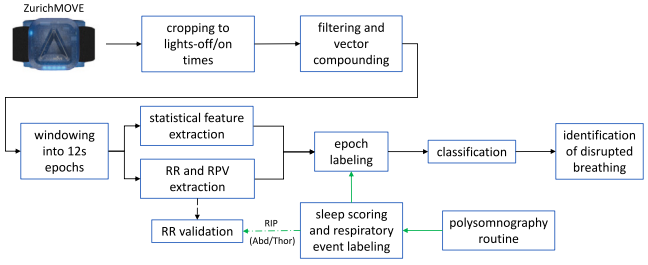

Fig. 3. Algorithmic flow diagram outlining the method to create the classification model to identify disrupted breathing. The polysomnography (PSG) signals (in green) are used as a reference for labeling the accelerometer data for training the model. As a separate outcome, the respiratory rate (RR) is validated using the respiratory inductance plethysmography (RIP) biosignals from the abdomen and thorax (Abd/Thor), available during the PSG routine.

(RIP) bands strapped around the thorax and abdomen, nasal flow and thermistor, and pulse oximetry. Sleep stages were analyzed with the accompanying RemLogic software suite and scored according to the standard criteria of the American Association of Sleep Medicine [27].

The PSG gold standard was used as a validation reference against the accelerometer sensing module as part of the custom-made ZurichMOVE inertial measurement unit (IMU) [28]. It is a 9-axis IMU wearable activity monitoring device. Here, we utilized the sensor at a chosen acceleration sensitivity of ±8 g and sampling rate of 50 Hz. It was strapped around the lower section of the sternum of each participant with an elastic strap. The ZurichMOVE sensor stored the acceleration data in a MATLAB-compatible file on an integrated SD card. The setup involving both the PSG device and accelerometer are illustrated in Fig. 1.

2.3. Signal pre-processing

The respiratory activity captured by the PSG was preliminarily scored using an automatic algorithm provided by RemLogic (the 'Respiratory Analyzer' tool). Using specifically the thoracic and abdominal RIP belts, the tool also calculates the RR, which is generated from the output respiratory effort signal and based on inspiratory peaks identified per minute (i.e. a bpm output), with a sampling frequency of 1 Hz. Apnea/hypopnea events are breathing cessations with a minimum length of 10 s [27]. To ensure encapsulation of these respiratory events, an epoch size (i.e. a time window of sleep) of 12 s was chosen as a basis for classification. In order to establish one RR value per epoch, the RR trace was extracted and down-sampled to $\frac{1}{12}$ Hz using the Kaiser window method which approximates an anti-aliasing low-pass filter. Additionally, all disrupted respiratory events (obstructive, central, and mixed apnea/hypopnea events) were manually verified and corrected by a qualified somnologist. All the events, and their corresponding timestamps and duration times, were exported with millisecond precision. All further signal processing methods were performed with MATLAB R2020a (MathWorks, Massachusetts, USA). For subjects S_05 and S_10, the PSG device was disconnected during the night. These missing epochs, and a single preceding and proceeding epoch, were excluded from the data set. Any remaining epochs for classification were characterized as true 'Time in Bed'.

The accelerometer data were initially cropped to the lights-off and lights-on times defined by the PSG data. Breathing activity is expected between 6–30 bpm during sleep [11,29], which corresponds to a frequency range of 0.1–0.5 Hz. Each axis of the accelerometer signal was passed through an order 29 zero-phase infinite impulse response (IIR) Butterworth high-pass filter with corner frequency 0.05 Hz, followed by an order 10 zero-phase IIR Butterworth low-pass filter with corner frequency 1.0 Hz. After filtering, the signal magnitude, $m(t)$, was computed (see Fig. 2). For each sample, the axes were vector compounded by computing the root mean square (RMS) of the respective axial components, such that:

$$m(t) = \sqrt{a_x^2(t) + a_y^2(t) + a_z^2(t)} \quad (1)$$

The signal magnitude was thresholded with an empirically estimated noise level and kept constant for all subjects. The signal was split into epochs of 12 s, and all proceeding calculations were carried out using these epochs. Fig. 3 outlines the overarching algorithm for our screening tool.

2.4. Estimating respiratory rate

2.4.1. Estimation

To calculate the accelerometer-based RR (RR_{Acc}) effectively, a 36 s range was considered. The peaks of the acceleration magnitude were

extracted in the time domain. The number of peaks found was summed over three epochs (i.e. the epoch of interest, as well as the preceding and proceeding epochs) with a total duration of 36 s (which was seen as the best-balanced approach to avoid having too large epoch sizes for identifying disrupted breathing versus sufficiently large epochs for calculating RR). The count was multiplied by a constant of $\frac{5}{3}$ to convert to the desired units of bpm, and applied as the RR_{Acc} for the central epoch of interest. Respiratory peaks were identified based on the reasonable assumption that no greater than eighteen peaks should physiologically be expected during sleep in 36 s, with at least 2 s of separation between them. The peaks were also thresholded to an empirically chosen noise level fixed at 0.004 g. Further algorithmic constraints included the maximum number of peaks with respect to 30 bpm (a reasonable assumption during sleep [11]), also enforcing a minimum distance between peaks on the same assumption, in order to further mitigate noise effects. Therefore, as outlined in Fig. 2, during regular breathing epochs an estimated breath is identified as the first valid peak of the 36 s range and then further peaks are identified at each inhalation/exhalation cycle. Where only two of three epochs were available for calculating the RR_{Acc} (at the start and end of the signal), the RR observations were carried forwards and backwards respectively.

2.4.2. Validation

To validate the RR estimation, we compared it on an epoch-to-epoch basis against the RR trace derived from the thoracic and abdominal RIP signals in the PSG routine (RR_{PSG}). RR_{PSG} is not available during detected body movement activity, and therefore such epochs were excluded from the validation of RR_{Acc}. Before down-sampling RR_{PSG} as part of signal pre-processing, the RR trace is calculated with integer precision. To conform with this, we therefore rounded the values of the RR_{Acc} and RIP-based RR_{PSG} signals to the nearest integers.

2.5. Feature set for respiratory activity

In order to automatically classify disrupted respiratory events during sleep, we designed a feature set, containing physiologically-motivated features from the RR calculator and established statistical features from both the time and frequency domains. During disrupted respiratory events, respiration is somewhat inhibited and often the movement of the thorax therewith. Inherently, we expect a reduced RR in epochs containing apnea events [2,27]. During transitions between regular and disrupted events, a large variance in inspiratory peak magnitudes is expected, and conversely a sustained low variance during disrupted breathing [11,30]. Based on this motivation, and the experience with feature extraction for respiratory effort signals from PSG and other contexts, such as cardiology [29,31], we earmarked the RR and RPV (respiratory peak variance) as potentially strong predictors of such disrupted respiratory events. We define the RPV as the variance of the signal magnitude for the set of respiratory peaks, $RR^p = (RR^p_1, \dots, RR^p_N)$, identified as part of the RR calculation:

$$RPV = var\left(\left[RR^p_1, \quad \dots, \quad RR^p_N\right]^T\right) \tag{2}$$

This is carried out over three consecutive epochs (as described for RR estimation), where RR^p_N is the last qualifying respiratory peak identified in the 36 s range. Similarly, the RR and RPV are assigned to the central epoch for the estimation outcome.

Further, using $m(t)$, we extracted ten time domain and four frequency domain features per epoch. The exception to this rule is the axes correlations, which are carried out using the filtered tri-axial components ($a_x(t)$, $a_y(t)$, $a_z(t)$). The non-normalized feature set, $q = (q_1, \dots, q_{16})$, was then normalized between the range of zero and one per feature, for all features in the set $f = (f_1, \dots, f_{16})$, such that f_i is the ith normalized feature of the sixteen final features, whereby:

$$f_i = \frac{q_i - min(q)}{max(q) - min(q)} \tag{3}$$

In order to calculate frequency domain features, the power spectral density estimate is carried out with a periodogram with a rectangular window of 1024 points for fast Fourier transform. In the specific case of the signal to noise and distortion ratio (SINAD) feature, this is provided in a non-logarithmic form (i.e. not in decibels, as usually prescribed) to avoid division by zero errors. The full set of features is described in Table 2.

2.6. Classification model

To classify breathing epochs as disrupted or regular, we used the labeling scheme available from the PSG scoring as the gold standard. Some post-processing was involved to associate event labels to the qualifying breathing epochs from the accelerometer data, such as when events were longer than one epoch's worth. Here, the label was applied to the epoch, or epochs, in question even when disrupted activity existed only in part of a full 12 s time span. From the labeling in RemLogic, we amalgamated all types of apnea/hypopnea events (central, obstructive, and mixed) into a disrupted class.

When considering an adult PSG routine, apnea events are defined by a drop of ≥90% in peak signal excursion for ≥10 s, whereas hypopnea events as only a drop of ≥30% for the same duration, relative to the pre-event baseline [27]. During obstructive apnea, a persistent and paradoxical respiratory effort is observed from both the abdominal and thoracic RIP signals with no constructive breathing patterns produced (when considering the sum of the RIP signals) [30,32]. Conversely, respiratory movements are characteristically lacking during central apnea events [32], with only an observable cardio-ballistic artifact usually remaining [33]. The signal profile of mixed apnea events initially suggest a central apnea cessation, followed by the thoracoabdominal pattern characteristic to obstructive apnea events [32]. Generally, the hypopnea events tend to maintain some regularity in breathing, but with a reduced signal excursion and, in the case of RIP, tidal volume [32]. Since the well-defined physiological characteristics of such respiratory events generally conform, the events can be considered independently in the classification approach, regardless of their frequency during the night. If no qualifying disrupted respiratory events were present within the epoch, it was labeled as regular. Fig. 4 provides representative samples of both classes of respiratory events. It is noteworthy that the accelerometer signal magnitude, $m(t)$, tends to mimic the sum of the magnitudes of the RIP signals.

For training, a total of 90.7 h of data was randomly partitioned (with stratification) without replacement, containing 90.3 h of regular, and 0.4 h of disrupted, epochs. To develop our final model, we

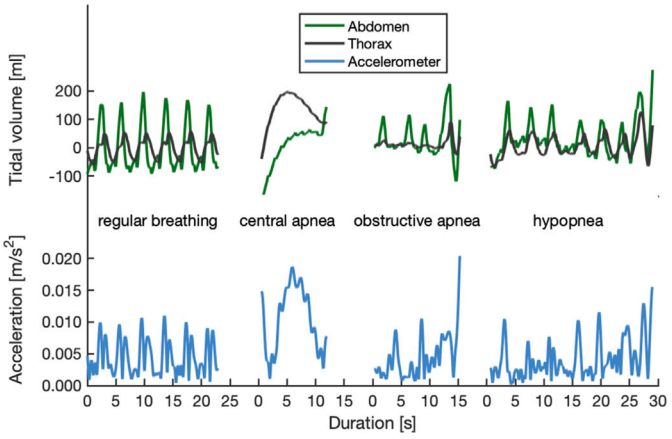

Fig. 4. Representative examples of regular breathing and disrupted respiratory events (central apnea, obstructive apnea, hypopnea) are shown. On the top, the PSG reference is shown as the RIP abdomen (green) and thorax (gray) signals. On the bottom, the filtered acceleration signal magnitude (blue) is indicated for the same time frames.

Table 2
Feature set.

Feature	Domain	Description
Respiratory rate (RR)	Time	Number of breaths per minute (bpm)
Respiratory peak variance (RPV)	Time	Variance of identified inspiratory peaks in the signal magnitude
Standard deviation	Time	Standard deviation of the signal magnitude
Variance	Time	Variance of the signal magnitude
Peak-to-peak difference	Time	Difference between max and min values of the signal magnitude
Peak-to-RMS ratio	Time	Ratio of signal magnitude peak value to the RMS value
Peak-to-average signal	Time	Peak to average signal magnitude ratio
Peak-to-average power	Time	Peak to average power ratio of the signal magnitude
Kurtosis	Time	"Tailed-ness" of distribution exhibited by the signal magnitude
x-y correlation	Time	Pearson correlation between RMS signals of x and y axes
x-z correlation	Time	Pearson correlation between RMS signals of x and z axes
y-z correlation	Time	Pearson correlation between RMS signals of y and z axes
Median frequency	Frequency	Median frequency of the signal magnitude's power spectrum
Mean frequency	Frequency	Mean frequency of the signal magnitude's power spectrum
SINAD	Frequency	Signal to noise and distortion ratio
Band-power	Frequency	Band-power of the spectrum of the signal magnitude

benchmarked two feature sets for classification: a subset containing only the two physiologically-motivated features (the RR and RPV), as well as a full set comprising all sixteen features. To outline the significance of solely these two features towards the full set, the *k*-NN classifier was used — a relatively straightforward supervised approach which clusters similar data points together [34]. In approaching the full set, the classifier harnesses the Random Undersampling Boosting (RUSBoost) ensemble learning meta-algorithm [35]. This is rooted in using Random Forests, which have fast training times and tend to avoid over-fitting [36]. We selected the RUSBoost classifier due to its ability to combat severe class imbalance in data sets by performing random undersampling, as well as applying boosting upon weak learners in the ensemble [35,37].

2.6.1. Validation

To validate the binary classification models, we performed a tenfold cross-validation. We enforced a stratification method to ensure that enough disrupted events were present in each fold, taking into account that data from individual subjects could not be completely separated between training and testing bins during cross-validation. In effect, the random partitioning and cross-validation combined mean that the model has no knowledge of to whom certain epochs of breathing belong to, and which subjects have a greater or lower level of respiratory disruption (i.e. their AHI scores). We performed an automated Bayesian optimization followed by a manual grid-search search for relevant hyper-parameter selection, using the average outcomes of the validation metrics based on the ten iterations.

2.6.2. Testing

For testing, we used data from the subject S_08, which is independent from the training (and cross-validation) data set. The test data set comprises 7.9 h of 'Time in Bed', including 6.7 h of regular epochs and 1.2 h of disrupted epochs. The size and nature of the test data set was chosen as a subject with a somewhat average night of sleep, and a heightened level of disrupted respiratory events in comparison to the folds in the cross-validation.

3. Results

3.1. Respiratory rate validation

We validated 89.4 h (26833 epochs) of RR data from twelve subjects as per Table 3. The RR_{PSG} trace for subject S_11 unfortunately could not be extracted for validation due to a timing malfunction between the PSG and accelerometer, and was only used as part of the classification analysis. 596 (2.17%) epochs were removed due to any movement events or PSG device disconnections (identified by an IMU posture sensor as part of the PSG setup). The results are outlined in Table 3, showing the mean for accelerometer and PSG-based estimations, difference of means, and standard deviation for each subject. Subject S_06 shows the most accurate RR_{Acc} results with a mean difference of +0.1 bpm, and subject S_02 the least accurate, with +4.6 bpm mean difference. In general, the standard deviations per subject for both PSG and accelerometer-based estimations are reasonably similar.

Table 3
Per subject outcomes for the respiratory rate validation (indicated with $\mu(\sigma)$, μ: mean value, σ: standard deviation; Δ: difference; $\Sigma(S)$ represents the sum over all subjects).

Subject	RR_{Acc}	RR_{PSG}	$\Delta(RR_{Acc} - RR_{PSG})$
S_01	14.6 (4.6)	18.0 (2.4)	−3.4
S_02	18.7 (3.3)	14.1 (1.8)	+4.6
S_03	17.6 (3.0)	18.8 (4.8)	−1.3
S_04	17.5 (1.8)	16.5 (2.5)	+1.0
S_05	17.2 (2.3)	16.0 (3.9)	+1.2
S_06	17.3 (1.5)	17.2 (2.1)	+0.1
S_07	17.3 (2.2)	15.7 (1.8)	+1.5
S_08	18.4 (2.2)	15.4 (3.4)	+3.0
S_09	16.7 (2.8)	15.8 (1.8)	+0.9
S_10	16.6 (5.4)	14.5 (1.9)	+2.1
S_12	16.6 (3.2)	17.5 (2.4)	−0.9
S_13	13.9 (4.1)	15.3 (2.2)	−1.4
$\Sigma(S)$	**16.9 (3.0)**	**16.2 (2.6)**	**1.8 (2.2)**

In the Bland–Altman plot [38] in Fig. 5, the assumed ground truth RR_{PSG} data points on the x-axis are compared against the difference of means between the RR_{Acc} and RR_{PSG} for each subject. All the subjects fall within the 95% limits of agreement of the Bland–Altman plot (±1.96 times the standard deviation), exhibiting a mean difference and standard deviation of +1.8 bpm and +2.2 bpm respectively. For further insight, Fig. 6 presents the distribution of RR estimations for each subject for both modalities, as well as an accumulated representation. The most populated histogram bin (16-18 bpm) is the same for both modalities overall, and is reasonably represented on an individual basis for most subjects. Subjects S_01, S_02, and S_08 exhibit large standard deviations between modalities. The data sets represent normal distributions according to the Shapiro–Wilk statistical test [39].

3.2. Classifying respiratory activity

After tuning the model appropriately, the final ensemble classifier was trained with 63 learners, maximum 18 splits, a learning rate of 1.0, and misclassification cost of 200. The classification outcomes for the test data set are shown in Table 4. In this study, we defined sensitivity as the probability of an epoch being identified as truly disrupted. Accordingly, we defined specificity as the probability of an epoch being identified as truly regular. An overall classification accuracy of 70.95% was achieved, with sensitivity and specificity of 76.05% and

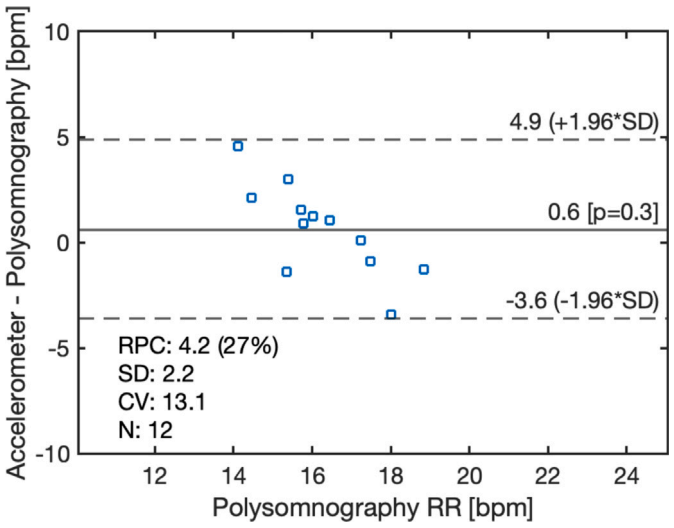

Fig. 5. Bland–Altman plot representing accelerometer-based versus polysomnography-based (respiratory inductance plethysmography) estimation of respiratory rate (RR) in breaths per minute (bpm) during 'Time in Bed' for twelve subjects, on a per subject basis (N = 12). The solid line indicates the mean difference, and the dotted lines represent the 95% limits of agreement (±1.96 times the standard deviation). RPC: reproducibility coefficient; SD: standard deviation; CV: coefficient of variation.

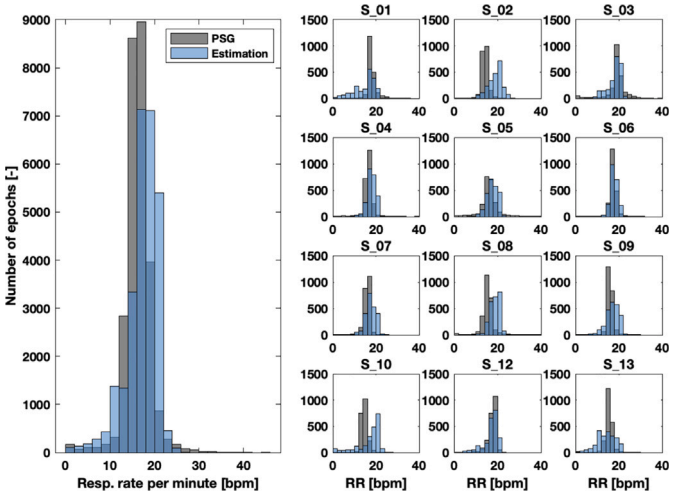

Fig. 6. Distribution of the respiratory rate (RR) estimations from the accelerometer (blue) and polysomnography gold standard (gray) are shown. On the left side, a histogram of the RR in breaths per minute (bpm) is shown from twelve healthy subjects over a total 89.4 h of recording. On the right, the distributions of the individual subjects are presented. In all cases, the histogram bins represent 2 bpm.

70.05% respectively. The prevalence was 15.03% in the test set. To further highlight the importance of the RR and RPV predictors, we also attempted classification solely with these two predictors, using the *k*-NN classifier [34] combined with 91 neighbors ($k = 91$), the Euclidean distance metric, and the same misclassification cost of 200. Exploiting all sixteen features instead of only the RR and RPV improves overall classification accuracy by over 2%, but the sensitivity by over 45%. Fig. 7 exemplifies the importance of the RPV towards the strength of the classification model. With a contribution of 67.16%, the RPV is considered over six times more important than the next best feature (the y-z correlation). The RR contributes 2.04% of variance in the classification model.

Table 4
Classification model outcomes for the test data set (PPV = positive predictive value, NPV = negative predictive value).

Feature set	Classifier	Sensitivity (%)	Specificity (%)	Accuracy (%)	PPV (%)	NPV (%)
RR and RPV	*k*-NN	30.36	75.96	69.11	18.26	86.05
All 16	RUSBoost	76.05	70.05	70.95	30.99	94.29

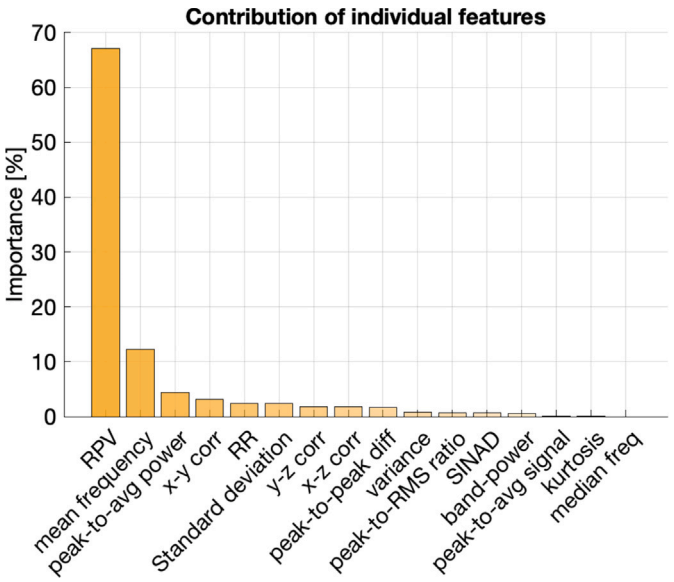

Fig. 7. Feature importance by percentage contribution in descending order in the RUSBoost classification ensemble model based on the cross-validation data discussed in Section 2.6.1. The respiratory peak variance accounts for 67.16% of importance in the model. The two physiologically-motivated features (RPV and RR) account for 69.20%.

4. Discussion

We investigated the potential of a chest-worn accelerometer sensor to unobtrusively measure RR during sleep, introduced a new physiologically-motivated feature set, and presented a classifier as a proof-of-concept to show that the feature set is able to detect disrupted respiratory activity, such as apnea/hypopnea events. With the data from the accelerometer sensor in our study, we reliably assessed the RR with a mean difference of 1.8 bpm, and a standard deviation of the difference of means of 2.2 bpm. This outcome is near to what is carried out in clinical routines, where visual integer-based counting of breaths is still the norm [40]. Further, its adequacy to be used as a feature to detect irregularities in breathing is shown in our classification model. The level of accuracy in our approach is well in line with findings reported in other validatory studies exhibiting short, exemplary signals while awake, or using accelerometer-based measures on other body parts. We showed that the RR estimation can be applied for a full night, aided by the sensor being attached in a more comfortable position.

Over a full night of sleep with an accelerometer sensor positioned on the suprasternal notch Morillo et al. reported on average −0.8 bpm, and maximum differences of +2.11/−3.05 bpm [11]. Jarchi et al. reported maximum mean differences of accelerometer-based RR estimated in ICU patients between 0.9–2.56 bpm [13]. With our sensor positioned on the sternum, we achieved a comparable mean difference. This suggests that our chosen sensor positioning on the sternum is similarly well-suited for capturing the physiological chest movements associated with breathing. The maximum differences, however, especially for high and low RRs, were higher. The maximal difference was seen in subject S_02 at 4.6 bpm, similarly followed by S_01 and S_08 — we see two possible explanations for these results. First, that in our implementation, the RR_{Acc} estimations were limited to the expected

physiological boundaries of 6–30 bpm. This was achieved by choosing the corresponding filter criteria, compounded by an upper limit on the RR calculator. Although this led to more robust results, the accelerometer-based method might be less sensitive to fast changes in RR. Second, we note that the RIP-based RR_{PSG} estimation performs questionably in the breathing extrema. Since the expected range should sit between 6-30 bpm [11] (even during apneic events [27]), and the PSG data sometimes output RR values beyond these limits, we would suggest that the accelerometer-based estimation generates more physiologically-relevant RR values in such gray areas of respiratory activity. Moreover, despite the IMU sensor being part of the PSG routine as standard, RemLogic provides no accuracy level in neither determining movement events nor posture in bed with this device [41]. Since the software rightly refrains from providing a RR value at such time-points, it cannot be inferred that all such activity has been excluded from the PSG data set, and subsequently the validation process, correctly. When manually observing samples of the video recording of subjects during sleep, it is clear residual movement artifacts surrounding PSG-defined movement events in bed are inherently uncontrollable, and since RR_{PSG} is calculated at these time-points, this could explain the respiratory activity recorded at greater than 30 bpm. Despite the aforementioned challenges imposed when using RIP belts as a RR reference for validation, it is still the most convenient and least invasive way to continuously monitor RR during the night without disturbing sleep [42].

Thereafter, we harnessed the RR to create a wider feature set tailored to detecting changes in respiratory activity. The classification model correctly detected disrupted respiratory events with an accuracy of 70.95%. To our knowledge, it is the first time that an accelerometer-based classification model is presented as being able to detect the presence of breathing cessations within individual epochs during sleep. The automatic 'Respiratory Analyzer' built into RemLogic for PSG sleep scoring provides an overall mean sensitivity of 93.8% with a full PSG setup [41]; here, we were able to achieve 76.05% with a straightforward setup. With our current implementation, differentiating between central or obstructive apnea/hypopnea is not feasible, but the model output provides the same level of generalization given by the AHI clinical standard. This underlines the potential of the presented approach as a screening tool.

Other researchers have used machine learning approaches to classify subjects into groups with respect to their symptom severity, but without detecting individual events, thus lacking the potential of providing information about the number, or temporal appearance, of individual events. Pépin et al., for example, used a head-mounted sensor to measure mandibular movements, and discriminated between subjects with and without pathological sleep disorders based on a Respiratory Disturbance Index of below five and above fifteen with an accuracy of 92% and 83% respectively [25,27]. No performance metrics were reported on the level of detecting individual respiratory events or epochs, which would allow for a more insightful comparison to our approach. In the same vein, Van Steenkiste et al. achieved an accuracy and sensitivity level of 72.8% and 58.4%, respectively, using bio-impedance signals from the chest. While this approach had the advantage of being able to discriminate between obstructive and central apnea/hypopnea types, we were able to outperform the overall detection of disrupted respiratory events. Also, a heuristic approach for event-based detection of irregular respiratory events was recently presented by Ferrer-Llouis et al. with promising sensitivity results [43].

The two physiologically-motivated features introduced in this work were key for the classification model. Namely, the respiratory peak variance (RPV) as the most predictive contributor, and the basis of its calculation by means of the respiratory rate (RR) feature. The RPV showed to be highly predictive in detecting disrupted respiratory events and accounted for 67.16% in overall classification contribution. The contribution of the RR was lower than expected at 2.04%, yet still more predictive than half of all the conventional statistical features used. A classifier based on a subset of only these two physiologically-inspired features still established an overall classification accuracy of 69.11% and identified one in three disrupted epochs correctly. This reflects the potential of the RR and RPV as features for machine learning models in the domain of respiratory analysis, and suggests that the feature set presented in this work would also be able to detect respiratory events in patients exhibiting clinically-relevant levels of SRBDs.

When interpreting the results, one should note that the classification model was trained on a relatively small data set of healthy subjects, where disrupted respiratory events were present occasionally. Only subject S_08 exhibited a near-to-moderate level of SRBDs (AHI = 14.8), which is just below the threshold of clinical relevance [11]; this subject was therefore chosen as the independent test subject. The relatively low PPV reflects this fact, as it takes the prevalence of the disrupted class into account. Thus, a high number of disrupted breathing epochs as predicted with the current model would lead to further clinical examination, whereas the high NPV would lend confidence that an epoch of breathing classified as regular indeed shows no cessations of interest. For a more realistic testing scenario, an increased number of subjects presenting an elevated AHI would be of value.

To combat the imbalanced classes in the training set we ensured that in each cross-validation partition, the same ratio of respiratory events were present (i.e. stratified cross-validation), taking into account that no complete separation of data from the individual subjects could be realized. When training a future model based on data from SRBD patients, this should be taken into account. Despite the restraints imposed by the data set, the algorithm was able to effectively handle the imbalanced classes and reliably detected disrupted respiratory events on a subject with a heightened AHI score. Additionally, we applied boosting methods to counteract the influence of weak learners within the ensemble. With the RUSBoost classification model, we were able to use imbalanced data sets for feature-based respiratory analysis. Deriving a clinically meaningful index – such as the Apnea-Hypopnea Index (AHI) – would be insightful. With the data presented here, however, we cannot directly map the disrupted epochs to such an index. This is due to the randomized and non-chronological nature of the training data set, where we cannot apply the notion of epochs in series to coalesce them into potential single disrupted respiratory events (which may span over several epochs). With the current model and setup, however, applying an assumption that the 'Total Sleep Time' is equal to the 'Time in Bed', the maximum AHI can be indicated. As emphasized earlier, with additional, non-randomized data, the temporal sequence would still remain intact, and the model could be trained on a one subject-per-fold basis. Thus, applying this classification model on data of an additional subject (not included in the training/validation and testing routine), would result in the number of detected respiratory events for this subject and, with temporal analysis, potentially indicate a more accurate AHI outcome. Moreover, it must be stressed that this study was conducted in a clinical sleep laboratory, i.e. in an artificial, well-controlled environment, where the subjects were well cared for and data collection was carefully monitored; the applicability of our screening tool in an unattended home setting still needs to be tested.

In future work, we envisage that the algorithm presented in this paper can be harnessed and validated against a more diverse data set containing subjects with varying AHI levels and moderate-to-severe SRBDs. In particular, more subjects should be included in the test routine to validate the performance of the model comprehensively. In addition, individual subjects can then be utilized as test data sets to provide independent AHI score outputs to complement the epoch-by-epoch analysis presented in this work. Further development could improve the RR estimation as basis for the feature selection, for example with a cycle-per-cycle estimation with dynamic window sizing. Furthermore, the binary model could be augmented into a multi-class classification approach, which would identify a specific apnea/hypopnea type exhibited within a respiratory epoch, or group of epochs in series. With such validatory efforts, an accelerometer-based multi-sensor setup could potentially be deployed as a home screening tool before inviting selected patients with suspected SRBDs for more resource-intensive PSG routines.

5. Conclusion

In this study, we have explored applying machine learning methods for feature-based respiratory analysis. We introduced a physiologically-motivated feature set capable of detecting and classifying disrupted respiratory events during sleep using a chest-worn accelerometer. We successfully demonstrated the potential of this respiratory feature set in a preliminary application with young healthy volunteers. In doing so, we also validated the use of a single accelerometer for RR estimation, as well as in identifying apnea/hypopnea events, which are an important subset of SRBDs. Our feature-based accelerometer approach supports the prospect of introducing a preliminary home screening tool for respiratory analysis before asking selected patients to use the resource-intensive facilities of a sleep laboratory.

CRediT authorship contribution statement

Franziska Ryser: Conceptualization, Investigation, Writing – original draft, Visualization. **Simon Hanassab:** Methodology, Software, Formal analysis, Writing – original draft. **Olivier Lambercy:** Writing – review & editing, Supervision. **Esther Werth:** Writing – review & editing, Resources, Funding acquisition. **Roger Gassert:** Conceptualization, Writing – review & editing.

Declaration of competing interest

The authors declare that they have no known competing financial interests or personal relationships that could have appeared to influence the work reported in this paper.

Acknowledgments

The authors thank E. Montvai, V. Boller, L. Makowski, G. Da Silva André, and A. Wachter for their support in subject recruitment and overnight data collection. This work was supported in part by the Swiss National Science Foundation under Grant 320030_160075 and the ETH Zurich Foundation, in collaboration with Hocoma AG.

References

[1] A.R. Fekr, M. Janidarmian, K. Radecka, Z. Zilic, A medical cloud-based platform for respiration rate measurement and hierarchical classification of breath disorders, Sensors 14 (6) (2014) 11204–11224.

[2] American Academy of Sleep Medicine, The International Classification of Sleep Disorders, Revised, American Academy of Sleep Medicine, Chicago, IL, 2005.

[3] V.K. Kapur, D.H. Auckley, S. Chowdhuri, D.C. Kuhlmann, R. Mehra, K. Ramar, C.G. Harrod, Clinical practice guideline for diagnostic testing for adult obstructive sleep apnea: an American Academy of Sleep Medicine clinical practice guideline, J. Clin. Sleep Med. 13 (3) (2017) 479–504.

[4] Z. Kaya, M. Kayrak, K. Demir, M. Gündüz, H. Alibasiç, M. Karanfil, H. Akilli, A. Aribaş, A. Tuncez, A. İçli, The relationship between white coat hypertension and sleep quality, Sleep Biol. Rhythms 12 (3) (2014) 203–211, http://dx.doi.org/10.1111/sbr.12070.

[5] J. Karimi, B.M. Asl, Automatic detection of non-apneic sleep arousal regions from polysomnographic recordings, Biomed. Signal Process. Control 66 (2021) 102394, http://dx.doi.org/10.1016/J.BSPC.2020.102394.

[6] Y. Taghizadegan, N.J. Dabanloo, K. Maghooli, A. Sheikhani, Obstructive sleep apnea event prediction using recurrence plots and convolutional neural networks (RP-CNNs) from polysomnographic signals, Biomed. Signal Process. Control 69 (2021) 102928, http://dx.doi.org/10.1016/J.BSPC.2021.102928.

[7] N.A. Collop, S.L. Tracy, V. Kapur, R. Mehra, D. Kuhlmann, S.A. Fleishman, J.M. Ojile, Obstructive sleep apnea devices for Out-Of-Center (OOC) testing: Technology evaluation, J. Clin. Sleep Med. 7 (5) (2011) 531–548, http://dx.doi.org/10.5664/JCSM.1328.

[8] A. Bates, M.J. Ling, J. Mann, D.K. Arvind, Respiratory rate and flow waveform estimation from tri-axial accelerometer data, in: 2010 International Conference on Body Sensor Networks, IEEE, 2010, pp. 144–150, http://dx.doi.org/10.1109/BSN.2010.50.

[9] P.D. Hung, Central sleep apnea detection using an accelerometer, in: ACM Int. Conf. Proc. Series, Association for Computing Machinery, 2018, pp. 106–111, http://dx.doi.org/10.1145/3232651.3232660.

[10] S.P. Preejith, A. Jeelani, P. Maniyar, J. Joseph, M. Sivaprakasam, Accelerometer based system for continuous respiratory rate monitoring, in: 2017 IEEE International Symposium on Medical Measurements and Applications (MeMeA), 2017, pp. 171–176.

[11] D.S. Morillo, J.L.R. Ojeda, L.F.C. Foix, A.L. Jiménez, An accelerometer-based device for sleep apnea screening, IEEE Trans. Inf. Technol. Biomed. 14 (2) (2010) 491–499.

[12] P.K. Dehkordi, M. Marzencki, K. Tavakolian, M. Kaminska, B. Kaminska, Validation of respiratory signal derived from suprasternal notch acceleration for sleep apnea detection, in: 2011 Annual International Conference of the IEEE Engineering in Medicine and Biology Society, 2011, pp. 3824–3827.

[13] D. Jarchi, S.J. Rodgers, L. Tarassenko, D.A. Clifton, Accelerometry-based estimation of respiratory rate for post-intensive care patient monitoring, IEEE Sens. J. 18 (12) (2018) 4981–4989.

[14] G.-Z. Liu, Y.-W. Guo, Q.-S. Zhu, B.-Y. Huang, L. Wang, Estimation of respiration rate from three-dimensional acceleration data based on body sensor network, Telemed. E-Health 17 (9) (2011) 705–711.

[15] P. Jiang, R. Zhu, Dual tri-axis accelerometers for monitoring physiological parameters of human body in sleep, in: 2016 IEEE SENSORS, IEEE, 2016, pp. 1–3.

[16] P. Kuwalek, B. Burlaga, W. Jesko, P. Konieczka, Research on methods for detecting respiratory rate from photoplethysmographic signal, Biomed. Signal Process. Control 66 (2021) 102483, http://dx.doi.org/10.1016/J.BSPC.2021.102483.

[17] A. Bricout, J. Fontecave-Jallon, D. Colas, G. Gerard, J.-L. Pépin, P.-Y. Guméry, Adaptive accelerometry derived respiration: Comparison with respiratory inductance plethysmography during sleep, in: 2019 41st Annual International Conference of the IEEE Engineering in Medicine and Biology Society (EMBC), IEEE, 2019, pp. 6714–6717.

[18] D. Waltisberg, O. Amft, D.P. Brunner, G. Troster, Detecting disordered breathing and limb movement using in-bed force sensors, IEEE J. Biomed. Health Inf. 21 (4) (2017) 930–938, http://dx.doi.org/10.1109/JBHI.2016.2549938.

[19] C.L. Bucklin, M. Das, S.L. Luo, An inexpensive accelerometer-based sleep-apnea screening technique, in: Proc. IEEE 2010 Nat. Aerospace Electronics Conf., 2010, pp. 396–399.

[20] P. Pierleoni, L. Pernini, A. Belli, L. Palma, Real-time apnea detection using pressure sensor and tri-axial accelerometer, in: IEEE-EMBS Int. Conf. on Biomedical and Health Informatics (BHI), IEEE, 2014, pp. 513–516.

[21] A. Angelucci, D. Kuller, A. Aliverti, A home telemedicine system for continuous respiratory monitoring, IEEE J. Biomed. Health Inf. 25 (4) (2020) 1247–1256, http://dx.doi.org/10.1109/jbhi.2020.3012621.

[22] M. Al-Mardini, F. Aloul, A. Sagahyroon, L. Al-Husseini, Classifying obstructive sleep apnea using smartphones, J. Biomed. Inform. 52 (2014) 251–259, http://dx.doi.org/10.1016/j.jbi.2014.07.004.

[23] B. Camcı, C. Ersoy, H. Kaynak, Abnormal respiratory event detection in sleep: A prescreening system with smart wearables, J. Biomed. Inform. 95 (2019) http://dx.doi.org/10.1016/j.jbi.2019.103218.

[24] T. Van Steenkiste, W. Groenendaal, P. Dreesen, S. Lee, S. Klerkx, R. De Francisco, D. Deschrijver, T. Dhaene, Portable detection of apnea and hypopnea events using bio-impedance of the chest and deep learning, IEEE J. Biomed. Health Inf. 24 (9) (2020) 2589–2598, http://dx.doi.org/10.1109/JBHI.2020.2967872.

[25] J.-L. Pépin, C. Letesson, N.N. Le-Dong, A. Dedave, S. Denison, V. Cuthbert, J.-B. Martinot, D. Gozal, Assessment of mandibular movement monitoring with machine learning analysis for the diagnosis of obstructive sleep apnea, JAMA Netw. Open 3 (1) (2020) e1919657.

[26] M.W. Johns, A new method for measuring daytime sleepiness: The epworth sleepiness scale, Sleep 14 (6) (1991) 540–545.

[27] R.B. Berry, R. Budhiraja, D.J. Gottlieb, D. Gozal, C. Iber, V.K. Kapur, C.L. Marcus, R. Mehra, S. Parthasarathy, S.F. Quan, et al., Rules for scoring respiratory events in sleep: update of the 2007 AASM manual for the scoring of sleep and associated events: deliberations of the sleep apnea definitions task force of the American Academy of Sleep Medicine, J. Clin. Sleep Med. 8 (5) (2012) 597–619.

[28] ZurichMOVE. URL www.zurichmove.com.

[29] G. Gutierrez, J. Williams, G.A. Alrehaili, A. McLean, R. Pirouz, R. Amdur, V. Jain, J. Ahari, A. Bawa, S. Kimbro, Respiratory rate variability in sleeping adults without obstructive sleep apnea, Physiol. Rep. 4 (17) (2016) e12949.

[30] M. Glos, A. Sabil, K.S. Jelavic, C. Schöbel, I. Fietze, T. Penzel, Characterization of respiratory events in obstructive sleep apnea using suprasternal pressure monitoring, J. Clin. Sleep Med. 14 (3) (2018) 359–369.

[31] T. Bhattacharjee, D. Das, S. Alam, M.V.A. Rao, P.K. Ghosh, A.R. Lohani, R. Banerjee, A.D. Choudhury, A. Pal, SleepTight: Identifying sleep arousals using inter and intra-relation of multimodal signals, in: 2018 Computing in Cardiology Conference (CinC), Vol. 45, IEEE, 2018, pp. 1–4, http://dx.doi.org/10.22489/CinC.2018.245.

[32] M.J. Tobin, M.A. Cohn, M.A. Sackner, Breathing abnormalities during sleep, Arch. Internal Med. 143 (6) (1983) 1221–1228.

[33] P.J. Simons, S. Overeem, Recording, analysis and interpretation, in: Sleep Disorders in Neurology: A Practical Approach, John Wiley & Sons, 2018, p. 16.

[34] N.S. Altman, An introduction to kernel and nearest-neighbor nonparametric regression, Amer. Statist. 46 (3) (1992) 175–185.

[35] C. Seiffert, T.M. Khoshgoftaar, J. Van Hulse, A. Napolitano, RUSBoost: Improving classification performance when training data is skewed, in: 2008 19th Int. Conf. on Pattern Recognition, 2008, pp. 1–4.
[36] L. Breiman, Random forests, Mach. Learn. 45 (1) (2001) 5–32.
[37] Y. Freund, R. Schapire, N. Abe, A short introduction to boosting, J.-Japan. Soc. Artif. Intell. 14 (771–780) (1999) 1612.
[38] J.M. Bland, D.G. Altman, Statistical methods for assessing agreement between two methods of clinical measurement, Lancet 327 (8476) (1986) 307–310, http://dx.doi.org/10.1016/S0140-6736(86)90837-8, Originally published as Volume 1, Issue 8476.
[39] S.S. Shapiro, M.B. Wilk, An analysis of variance test for normality (complete samples), Biometrika 52 (3/4) (1965) 591–611.
[40] J. Mann, R. Rabinovich, A. Bates, S. Giavedoni, W. MacNee, D. Arvind, Simultaneous activity and respiratory monitoring using an accelerometer, in: 2011 Int. Conf. on Body Sensor Networks, IEEE, 2011, pp. 139–143.
[41] RemLogic 3.4 Instructions for Use, Embla Systems, 2016.
[42] H. Liu, J. Allen, D. Zheng, F. Chen, Recent development of respiratory rate measurement technologies, Physiol. Meas. 40 (7) (2019) http://dx.doi.org/10.1088/1361-6579/ab299e.
[43] I. Ferrer-Lluis, Y. Castillo-Escario, J.M. Montserrat, R. Jane, Analysis of smartphone triaxial accelerometry for monitoring sleep-disordered breathing and sleep position at home, IEEE Access 8 (2020) 71231–71244, http://dx.doi.org/10.1109/ACCESS.2020.2987488.